

Applications of Muography to the Industrial Sector

P. Martínez Ruiz del Arbol,¹ Aitor Orio Alonso,² Carlos Díez,² and Pablo Gómez García²

¹*Instituto de Física de Cantabria, Avda Los Castros s/n, 39005, Santander, Spain*

²*Muon Tomography Systems S.L., Bizkaia, Spain*

Corresponding author: P. Martínez Ruiz del Arbol

Email: parbol@ifca.unican.es

Abstract

Muography can be exploited as a Nondestructive Testing technique to perform preventive maintenance of equipment and production process control in the context of the industry. The large penetration power of the muon radiation and the capability to operate the detectors without physical contact with the facility offer unique possibilities for a large variety of industrial problems. At the same time, most of the industrial applications of muography can use engineering drawings of the equipment in such a way that only the detection of small variations with respect to that equipment is pursued. This strongly reduces the mathematical complexity of the imaging algorithms. Several used cases of muography in the industry are reviewed in this paper.

Keywords: muography, muon tomography, industrial application, nondestructive testing

DOI: 10.31526/JAIS.2022.267

1. INTRODUCTION

The processing of raw materials requires the installation of large facilities with equipment such as furnaces, cauldrons, and pipes. This equipment is usually arranged in large factories in which several chemical, electrical, or mechanical processes occur in a sequential mode transforming the raw input into the desired product. Industrial companies spend millions of Euros every year in order to perform maintenance of the equipment and control of the production processes. There is a large variety of different techniques that can be applied to fulfill these tasks. Most of them are framed in the context of the so-called Nondestructive Testing (NDT) techniques, which allow performing an inspection of the facilities without damaging the equipment. Muography can be operated as a new NDT for specific problems where other NDTs offer poor results. The use of muon radiation offers unique potential to inspect large equipment such as furnaces or cauldrons where other NDTs are lacking penetration power. Muography also allows performing an inspection without touching the surfaces of the equipment, opening the possibility of operating, while the factory is in production. Finally, since muography does not require any radiation protection control, it can be operated in a cheap and safe way, allowing even the application of permanent installations to perform continuous monitoring.

2. COMMON FEATURES OF INDUSTRIAL APPLICATIONS OF MUOGRAPHY

The number of possible applications of muography to the industrial sector is quite large since there is a wide heterogeneity of problems and challenges. Nevertheless, there are several common aspects shared by most of the use cases. The dimensions of the objects typically range from a few tenths of cm to a few m, and the most common materials are steel, concrete, refractory, and carbon. The environment surrounding the equipment is usually quite packed with concurrency of other equipment, scaffolding, and service structures. This often imposes tight constraints on the possible locations of the muon detectors. The temperature and humidity conditions can be usually relatively high (up to 60°C and above 80%) due to the residual heat irradiated by the equipment and the possible evaporation processes taking place during production processes. The atmosphere can be dirty, containing particles and dust in suspension. Muon detectors need to be conveniently isolated to be able to operate in these conditions. In many used cases, there are also time restrictions in the sense that exposure times are limited by the natural times of the production processes.

Muography applications in this context share also an important feature from the algorithmic point of view: in most of the cases, detailed drawings of the equipment including densities and dimensions are available. The imaging algorithms do not need to infer the full geometry of the system, as other muography algorithms do [1, 2, 3], but simply to find small variations on top of the nominal design. In practice, this means that the complexity of the problem can frequently be reduced to a small set of parameters, opening the possibility of using parametric estimation methods or simple regression techniques including those based on Machine Learning techniques.

In order to illustrate these features, the problem of the ladle furnace is considered. Ladle furnaces are used in the heavy industry to transport melted minerals from some locations of the facility to others. The exact amount of melted material in a ladle is hard to estimate since an opaque, several-cm-thick layer of slag appears on top of the mineral. A possible muography-based solution

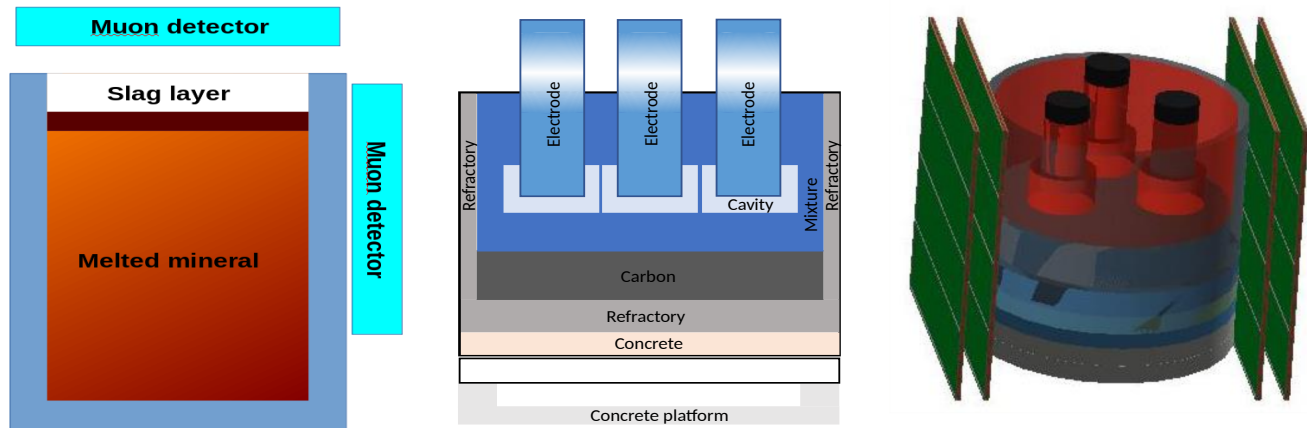


FIGURE 1: Diagram of a possible scattering muography setup to estimate the thickness of the slag layer on top of the mineral mixture in a ladle furnace (left). Sketch of a generic electric arc furnace with three carbon electrodes (middle) and GEANT4 tridimensional model with muon detectors at the sides (right).

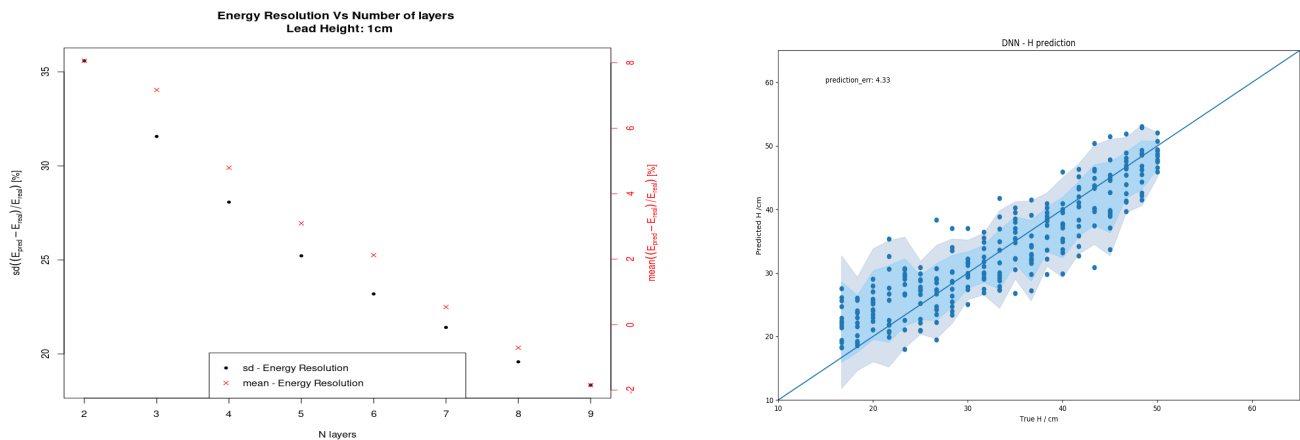


FIGURE 2: Evolution of the momentum resolution as a function of the number of extra layers used in the scattering energy determination system (left). Distribution of the measured h values as a function of the actual h value. The process is repeated for a number of statistically independent samples for a given h scenario (right).

could use two muon detectors installed on an L-shape as sketched in Figure 1(left), to perform scattering muography on the region covering the interface of the melted mineral and the slag layer. This detector configuration might be complicated since the upper detector has to be installed over the ladle requiring some kind of supporting structure. At the same time, the temperature in the surroundings of the ladle can be up to 60°C depending on the exact distance to the ladle. The atmosphere, especially in the region of the upper chamber, can contain gases emerging from the mixture including N_2 , CO_2 , CO , H_2 , and H_2O . Finally, the exposure time for a given measurement has to be limited to a few minutes in order not to affect the pace of the production process of the factory.

3. POSITIONING OF CARBON ELECTRODES IN ELECTRIC ARC FURNACES

Electric arc furnaces are another kind of devices used frequently in different factories. These instruments are composed of a vessel of refractory and other materials heated by the electric current flowing through the carbon-based electrodes introduced in the mixture. Figure 1(middle) shows a drawing of a generic electric arc furnace with a three-electrode configuration. The dynamics of the electric arc furnaces are complex and exhibit behaviors that are not fully understood nowadays. The exact position of the electrodes is suspected to have an impact on the efficiency of the chemical reactions taking place in the region below. On the other hand, the distance, h , between the bottom of the furnace and the lower surface of the electrodes is hard to estimate and remains unknown in most of the current furnaces.

A scattering muography setup has been proposed in order to estimate the distance h . A full GEANT4 [4] model of an electric arc furnace has been built taking into account the main elements of the vessel structure, the electrodes, and the mixture, using the dimensions and densities provided by industrial partners. Figure 1(right) shows a view of this GEANT4 model including also

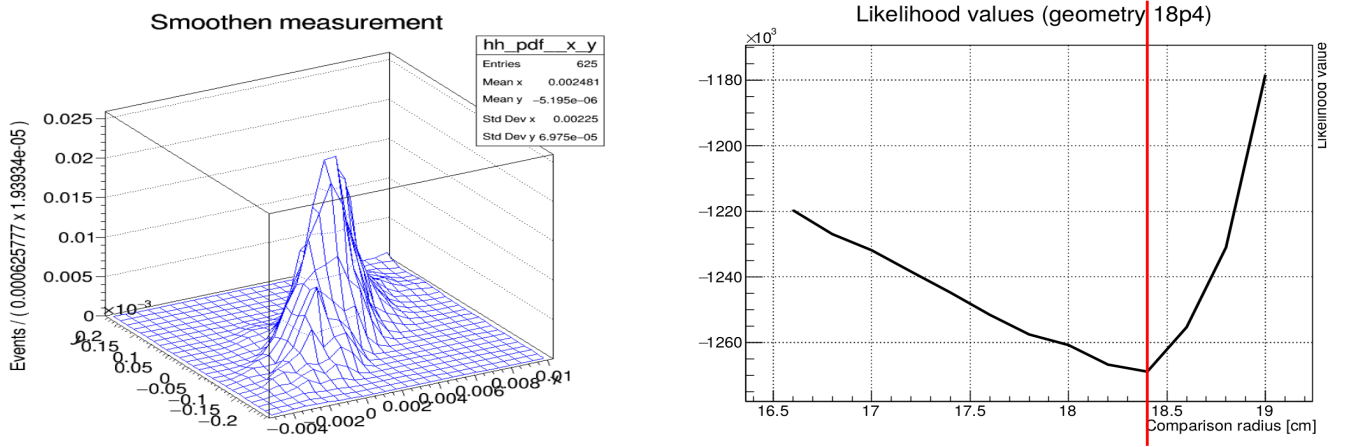


FIGURE 3: Fitted distribution of the Δx and Δvx variables using a KDE method (left). Shape of the $q = -2 \log(L)$ statistic for a pipe with an actual inner radius of 18.4 cm (right).

muon detectors based on multiwire proportional chambers as the ones owned by the company Muon Tomography Systems. The detector of the incoming trajectory has 3 detecting layers in both the x and y coordinates, the detector of the outgoing trajectory has also 3 detecting layers, but it is complemented with more layers in order to estimate the energy. Several scenarios have been defined according to different values of h . The CRY [5] simulator has been used in order to produce muon scattering datasets for each scenario.

The spatial coordinates of the incoming muons are noted as x_{in} , y_{in} , and z_{in} , with the z axis being orthogonal to the surface of the detector and vx_{in} and vy_{in} as the x and y coordinates of the normalized velocity vector. The coordinates of the outgoing muons are denoted as x_{out} , y_{out} , z_{out} , vx_{out} , and vy_{out} , respectively. These coordinates are transformed in such a way that the final datasets are composed of the variables associated with the incoming muons and the difference between the angles of the outgoing and incoming muons, the difference between the extrapolation of the trajectory of the incoming muon to the second detector assuming a straight line, and the spatial coordinates of the outgoing muons, denoted as Δvx , Δvy , Δx , and Δy .

Before performing the analysis on the furnace geometry, a system to estimate the energy of the muons is tested. The system uses the angular and position coordinates of the outgoing muons when crossing the additional layers of detection. A passive layer of lead with known thickness is sandwiched between every two detectors. The angular and spatial deviations between the layers are used as the input of a neural network performing a regression to the momentum of the muon. Figure 2(left) shows the resolution achieved on the momentum energy as a function of the number of layers.

The energy measurement for every muon is combined with Δx , Δy , Δvx , and Δvy in order to produce new composite variables. The distributions of the single and composite variables are then transformed into a tuple of numbers corresponding to the n -quantiles and used as the input for a Deep Neural Network performing a regression to the value of h . Figure 2 shows the results on the regression of the position of the electrodes for a test sample. The resolution achieved is of the order of 4 cm, representing a very valuable piece of information for the furnace operators. This method is currently being tested in a real environment in a factory in Spain.

4. ESTIMATION OF THE WEAR OF THERMALLY INSULATED INDUSTRIAL PIPES

The degradation of the inner walls of industrial pipes is a general problem in a large variety of factories and plants. Several NDT techniques [6, 7, 8] are frequently used to perform this task although many of them lose efficacy when the pipes are insulated with layers of rock-wool in order to keep the heat of the liquid or gas flowing through it. Scattering muography can be applied in this context by placing muon detectors on top and below a given section of the pipe. This problem has been addressed in the past using very simple statistical-comparison algorithms [10]. Two more sophisticated algorithms have been tested in order to infer the actual inner radius of the pipe with higher precision.

The first approach is based on a maximum-likelihood estimation. Every incoming trajectory measured in the upper detector is propagated in simulation a number of times and for a given inner radius scenario. A 2D histogram indicative of the spatial and angular deviations of every muon in the lower detector is obtained from this procedure and smoothed using a 2D Kernel Density Estimation (KDE) fit. This distribution is interpreted as a Probability Density Function (pdf), denoted as g_i , for every muon, and used to evaluate the actual deviation measurements. This information is combined for all the muons in order to build a likelihood depending on the inner radius of the pipes.

$$r_{\text{result}} = \arg \max_r \{-2 \log \mathcal{L}\} = \arg \max_r \left\{ -2 \log \sum_i g_i(\vec{r}_{in}, \vec{v}_{in}, \vec{r}_{out}, \vec{v}_{out}; r) \right\}. \quad (1)$$

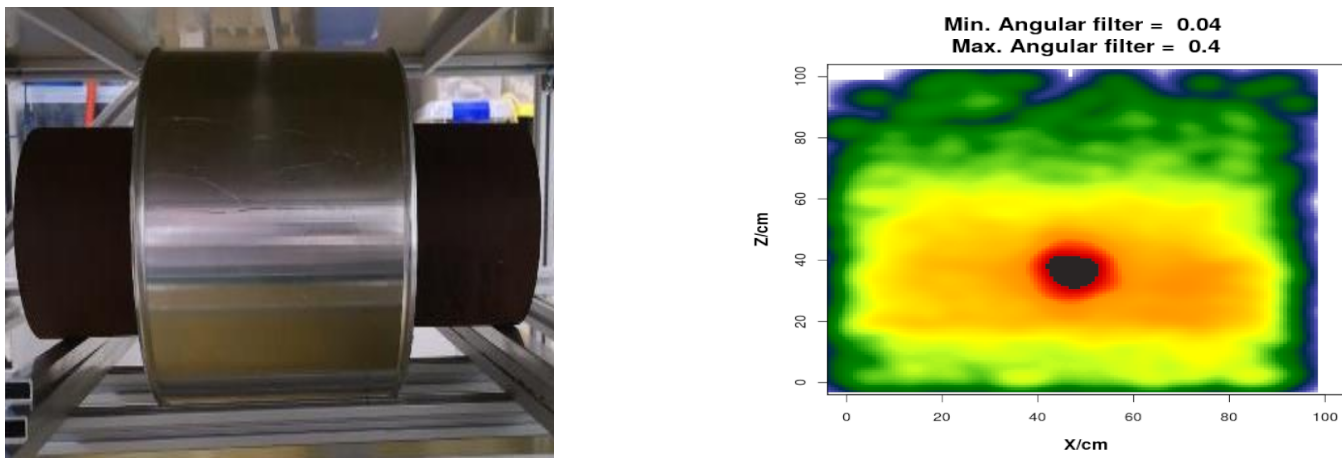


FIGURE 4: A section of a steel pipe with an insulator cover located between the muon detectors (left). POCA image showing the frontal view of the pipe. The red area corresponds to the steel wall of the pipe (right).

Figure 3(left) shows the KDE fit for one of the muons on a given dataset. Figure 3(right) shows the likelihood function for a case in which a steel pipe of 20 cm with a thickness of 18.4 cm is considered. This procedure is able to determine the real thickness of the pipes with a precision of about 2 mm using datasets corresponding to an exposure time of 15 minutes.

The second approach uses a very different methodology. The starting point of this algorithm is the Point-Of-Closest-Approach (POCA) method, which is applied to both real and simulated data in order to produce density maps of the pipes. These images are then used to train a Convolutional Neural Network (CNN) performing a regression to the inner radius of the pipes. The CNN uses a RESNET architecture [11] with 50 layers and it is pretrained using the ImageNET image dataset [12]. On top of this, the CNN is trained using POCA images corresponding to 15 minutes of exposure time with the Muon System detector configuration and for several thickness scenarios. Figure 4(left) shows a picture of one of the tested insulated pipes, while Figure 4(right) shows the corresponding POCA image used to feed the CNN. This algorithm provides a precision of about 2 mm in the estimation of the inner radius.

5. MUON DETECTORS FOR APPLICATION IN THE INDUSTRY

The detection technology used for the application of muography to the industrial sector is driven by three main factors: the cost of the detectors, the intrinsic resolution, and the robustness to operate in harsh environments. A good balance among the three is found in multiwire proportional chambers (MPCs).

This technology is slightly more complex to implement than other common technologies like scintillation detectors and is more sensitive to environment conditions like temperature or pressure. On the other hand, MPCs offer a good spatial resolution with high efficiency, they can be easily isolated from the environment, and they are lightweight and have a lower cost per electronic channel than other detection technologies. In addition, they present good resistance to mechanical vibrations and are easily repairable.

Figure 5 shows a picture of the setup used for most of the studies presented in this work. The detector consists of 3 sensitive layers with a surface of $1\text{ m} \times 1\text{ m}$. Each of the layers is composed of two sublayers of wires located orthogonal to each other in order to measure both the X and Y coordinates. The wires are separated by a distance of 4 mm and are embedded in a mixture of argon-CO₂. A power module provides high voltage to the wires and the power supply to the readout electronics. A master electronic module stores the information when a configurable number of layers have acquired a signal in a given time window. The final data stream is taken for storage using a simple USB connection. Detecting layers work in a modular way and can be expanded by connecting additional layers to cover more surfaces. The whole system can work autonomously by means of a conventional battery and a gas bottle. Each of the layers is inserted inside a hermetic methacrylate box to isolate them from the environment.

6. CONCLUSIONS

Muography can be used as a Nondestructive Testing technique to perform preventive maintenance of industrial equipment and monitoring of the production processes. Industrial problems present a key advantage with respect to other muography applications: the geometry and densities of the target objects are known nominally with high precision, meaning that the problem can be reduced to the estimation of a few parameters. On the other hand, the operation of muon detectors in industrial environments can be complicated because they usually have space and time restrictions and also relatively extreme atmospheric conditions in terms of humidity, temperature, and the presence of dust and/or gases. This paper presents two possible applications of muography being tested currently by the company Muon Systems in collaboration with other industrial partners. The first consists of the estimation of the position of the electrodes inside electric arc furnaces, and the second consists of the measurement of the level of degradation of the inner walls of thermally insulated pipes.

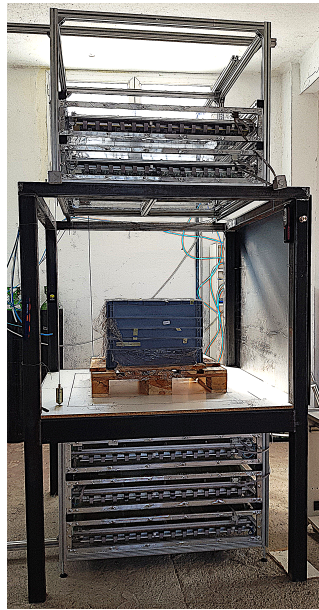


FIGURE 5: Full setup of MPC-based muon detectors for scattering muography operation.

CONFLICTS OF INTEREST

The authors declare that there are no conflicts of interest regarding the publication of this paper.

References

- [1] W. C. Priedhorsky, K. N. Borozdin, G. E. Hogan, C. Morris, A. Saunders, L. J. Schultz, and M. E. Teasdale. Detection of high-Z objects using multiple scattering of cosmic ray muons. *Rev. Sci. Instrum.* 74, 4294–4297 (10.1063/1.1606536), 2003.
- [2] L. J. Schultz, G. S. Blanpied, K. N. Borozdin, A. M. Fraser, N. W. Hengartner, A. V. Klimenko, and M. J. Sossong. Statistical reconstruction for cosmic ray muon tomography. *IEEE Trans. Image Process.* 16, 1985–1993 (10.1109/TIP.2007.901239), 2007.
- [3] L. J. Schultz, K. N. Borozdin, J. J. Gomez, G. E. Hogan, J. A. McGill, C. L. Morris, and M. E. Teasdale. Image reconstruction and material Z discrimination via cosmic ray muon radiography. *Nucl. Instrum. Methods Phys. Res. A, Accel. Spectrom. Detect. Assoc. Equip.* 519, 687–694 (10.1016/j.nima.2003.11.035), 2004.
- [4] S. Agostinelli, J. Allison, K. Amako, J. Apostolakis, H. Araujo, P. Arce, and D. Zschiesche. GEANT4—simulation toolkit. *Nucl. Instrum. Methods Phys. Res. A, Accel. Spectrom. Detect. Assoc. Equip.*, 506, 250–303 (10.1016/S0168-9002(03)01368-8), 2003.
- [5] H. Chris, L. David, and Verbeke D. W. Jerome. Cosmic-ray Shower Library (CRY). Retrieved 22 June 2018. See https://nuclear.llnl.gov/simulation/doc.cry.v1.7/cry_physics.pdf, 2012.
- [6] M. Twomey. Inspection techniques for detecting corrosion under insulation. United States: N.p., Web., 1997.
- [7] A. V. Bray, C. J. Corley, R. B. Fischer, J. L. Rose, and M. J. Quarry. Development of guided wave ultrasonic techniques for detection of corrosion under insulation in metal pipe. Paper presented at Proc. of the 1998 ASME Energy Sources Technology Conf, Houston, TX, USA Office of Scientific and Technical Information, US Department of Energy, 31st Dec. 1999.
- [8] H. Kwun and A. E. Holt. Feasibility of under-lagging corrosion detection in steel pipe using the magnetostrictive sensor technique. *NDT&E Int.* 28, 211–214 (10.1016/0963-8695(95)00019-T), 1995.
- [9] J. Bailey, N. Long, and A. Hunze. Eddy current testing with Giant Magnetoresistance (GMR) sensors and a pipe-encircling excitation for evaluation of corrosion under insulation. *Sensors* 17, 2229 (10.3390/s17102229), 2017.
- [10] P. Martinez Ruiz del Arbol et al., *Philos. Trans. A Math. Phys. Eng. Sci.* 2019 Jan 28; 377(2137): 20180054, doi: 10.1098/rsta.2018.0054.
- [11] Kaiming He, Xiangyu Zhang, Shaoqing Ren, and Jian Sun. Deep Residual Learning for Image Recognition, *Proceedings of the IEEE Conference on Computer Vision and Pattern Recognition (CVPR)*, 2016, pp. 770–778.
- [12] J. Deng, W. Dong, R. Socher, L.-J. Li, K. Li, and L. Fei-Fei, *ImageNet: A Large-Scale Hierarchical Image Database*, *IEEE Computer Vision and Pattern Recognition (CVPR)*, 2009.